

Talbot solitons

Oren Cohen,^{1,2,*} LipFah Chong,³ Tal Schwartz,² Tenio Popmintchev,¹ Margaret M. Murnane,¹ and Henry C. Kapteyn¹

¹JILA and Department of Physics, University of Colorado, Boulder, Colorado 80309-0440, USA

²Physics Department, Technion—Israel Institute of Technology, Haifa 32000, Israel

³Institute of Material Research Engineering, A*STAR 3 Research Link, Singapore 117602

*Corresponding author: coheno@colorado.edu

Received January 3, 2008; accepted February 16, 2008;
posted March 7, 2008 (Doc. ID 91317); published April 11, 2008

We propose a new type of scalar wave-mixing optical solitons, Talbot solitons. The soliton consists of sinusoidal and uniform components that are mutually coherent and jointly trapped in one direction. The intensity structure of the soliton oscillates in the propagation direction as a result of the linear Talbot effect and periodic nonlinear energy exchange between the components. Talbot solitons induce a 1D waveguide and a 2D photonic lattice within the waveguide that may be used for quasi-phase matching of frequency conversion and as a tunable waveguide filter. © 2008 Optical Society of America

OCIS codes: 190.6135, 190.3270, 190.4223.

Stripe beams in a bulk (3D) self-focusing nonlinear media suffer from transverse instability (TI), perturbations along the transverse uniform dimension of the beam, x , grow along the propagation, and the beam eventually disintegrates into an array of 2D filaments with a characteristic length between adjacent spots, l_{TI} [1]. This TI is especially severe in the case of a Kerr nonlinearity, prohibiting uniform stripe-shaped coherent solitons. Nonetheless, in 1985 Barthelemy *et al.* [2] devised a scheme to significantly suppress TI. In their method, the stripe beam is first evenly split into two stripes that are launched into the nonlinear crystal at the same position but at opposite angles, $\pm\theta$, relative to the propagation axis z . The beams interfere and produce a joint sinusoidal field along x . The TI is suppressed when the periodicity of the interference pattern is much smaller than l_{TI} of the nonsplit beam. In this way, Barthelemy *et al.* [2] demonstrated the first optical spatial solitons in Kerr media. Later, partially coherent stripe solitons [3] and necklace solitons [4] were also shown to be stable in Kerr media. The geometry of two copropagating mutually coherent waves was also employed for holographic solitons in photorefractives [5–7]. Notably, even though the two components nonlinearly interact, the intensities in all of these two-wave wave-mixing solitons, as well as the power in each of their constituents, are stationary along the propagation direction. In addition, the two mutually coherent wave geometries were extended to the counterpropagating geometry [5–12]. In this case, linear interference between the components leads to modulation of the total intensity. Still, the power in each component is conserved; there is no net energy exchange between the two components.

Here, we extend the mutually coherent wave-mixing soliton scheme to a three-wave-mixing scheme. We propose a soliton that consists of three stripe beams. Two fields propagate at $\pm\theta$ (their superposition being a sinusoidal field), and the third field propagates at $\theta=0$. The joint propagation of the sinusoidal and uniform waves results in a spatial Talbot effect; the intensity pattern of the soliton periodically

oscillates along the propagation direction. In addition, we find that the nonlinear wave mixing between the three waves leads to periodic energy exchange between them with periodicity that corresponds to half the Talbot distance. Nevertheless, the mutual trapping of the components results in a stable soliton. Finally, we discuss the potential applications of the waveguides and photonic lattices that are induced by Talbot solitons.

The intensity modulations owing to the Talbot effect, and the energy flow between the components, leads to modulations in the nonlinear induced index change along z . Often, such variations are destructive for solitons. However, if the intensity modulation length (Talbot distance) is much smaller than the diffraction and focusing lengths, then the effect of the intensity modulation is averaged to zero and solitons can exist [5–12].

The propagation of the slowly varying amplitude in nonlinear Kerr media can be described by the normalized cubic nonlinear Schrödinger equation (NLSE)

$$i \frac{\partial \Psi}{\partial z} + \frac{\partial^2 \Psi}{\partial x^2} + \frac{\partial^2 \Psi}{\partial y^2} + |\Psi|^2 \Psi = 0. \quad (1)$$

A self-trapped solution of Eq. (1) is given by $\Psi = \Psi_0 \operatorname{sech}(\Psi_0 y / \sqrt{2}) \exp(i\Psi_0^2 z / 2)$, where Ψ_0 is constant. This solution, which describes a stripe beam that is uniform in x and self-localized in y , suffers from TI. Perturbations along x grow with propagation distance, and the beam eventually disintegrates into an array of 2D filaments with a characteristic length between adjacent spots, l_{TI} [1]. To overcome this problem, Barthelemy *et al.* [2] replaced the uniform x dependence with a sinusoidal one, which eliminates the amplification of large wavelength perturbations that would otherwise break the uniform stripe beam. An approximate solution to the wave function of these solitons is given by

$$\Psi = \Psi_0 \sec h(\Psi_0 y \sqrt{3/8}) \cos(kx) \exp[i(3\Psi_0^2/8 - k^2)z], \quad (2)$$

where $k = \sin(\theta)/2$ is the transversal wave vector. We obtain Eq. (2) by transforming the large radius necklace solitons in [4] to a Cartesian coordinate system. We note that in these solitons, the induced index grating gives rise to holographic focusing [5,9] that increases the total self-focusing effect and is responsible for the replacement of the factor $\sqrt{1/2}$ in Eq. (2) by $\sqrt{3/8}$. Clearly, the intensity profile of the soliton is independent of z . This situation will be changed if another wave with a different wavenumber is added to the beam.

We derive the set of equations that describe Talbot solitons. Let the scalar slowly varying envelope be written as $\Psi(x, y, z) = \Phi_1(y, z) + \Phi_2(y, z) \cos(kx)$, where $\Phi_1(y, z) = \phi_1(y, z) \exp(i\alpha_1 z)$ and $\Phi_2(y, z) = \phi_2(y, z) \exp(i\alpha_2 z)$ are the uniform and sinusoidal complex envelopes, respectively; $d = 2\pi/k$ is the periodicity of the sinusoidal component; and $\phi_{1,2}$ and $\alpha_{1,2}$ are real functions and the propagation wavenumbers, respectively. The Talbot distance, after which the field reconstructs itself, is $\Lambda_T = 2\pi/\delta$, where $\delta = \alpha_1 - \alpha_2$. Inserting the above ansatz into Eq. (1) and selecting synchronous terms results in

$$i \frac{\partial \Phi_1}{\partial z} + \frac{\partial \Phi_1}{\partial y^2} + \left[\phi_1^2 + \frac{\phi_2^2}{2} \right] \Phi_1 = -2\phi_1 \phi_2 \cos(\delta z) \frac{\Phi_2}{2}, \quad (3a)$$

$$i \frac{\partial \Phi_2}{\partial z} + \frac{\partial \Phi_2}{\partial y^2} + \left[\phi_2^2 + \frac{3\phi_1^2}{4} - k^2 \right] \Phi_2 = -2\phi_1 \phi_2 \cos(\delta z) \Phi_1. \quad (3b)$$

The terms in the square brackets, and the right-hand terms in Eqs. (3a) and (3b), describe joint focusing and energy transfer between the components, respectively. We first analyze the energy exchange by neglecting the diffraction (second terms) and joint focusing (square brackets). Employing the conservation of energy $C = \phi_1^2 + \phi_2^2/2$ we get

$$\phi_1(z)^2 = \phi_1(0)^2 CG / [\phi_2(0)^2 + \phi_1(0)^2 G], \quad (4)$$

where $G = \exp\{C[1 - \cos(2\delta z)]/\delta\}$. Equation (4) is periodic in z with periodicity that corresponds to half the Talbot distance. We tested the analytic model by simulating the propagation of the initial beam $\Psi(z=0, x) = \phi_1(0) + \phi_2(0) \cos(kx)$ using the (1+1) D NLSE [Eq. (1) without the third term] with $\phi_1(0) = 0.2$. Figure 1(a) shows the maximum normalized energy flow (i.e., $\max[\phi_1(z)/\phi_1(0)]$) for the broad region of $d = 2\pi/k$ and $\phi_2(0)$ in which Eq. (4) matches the simulated results very well. An example with $\phi_2(0) = 1$ and $d = 0.5$ is shown in Figs. 1(b)–1(d). The Talbot distance is $\Lambda_T \approx 0.04$, which matches the linear case ($\Lambda_T = d^2/2\pi \approx 0.04$). In other words, the Talbot distance in this parameter range is approximately independent of the intensity (the Talbot distance gets shorter when the intensities are larger). Also, note

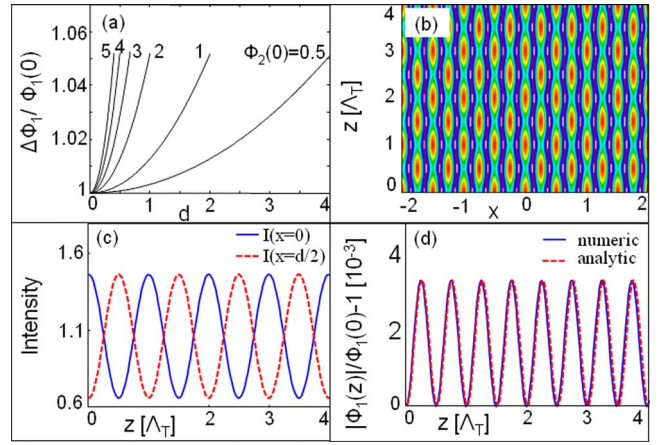


Fig. 1. (Color online) Talbot effect in (1+1) D nonlinear Kerr medium. (a) Maximum increase in the amplitude of the uniform field, normalized by its initial amplitude, as a function of the periodicity of the sinusoidal field. (b) Intensity versus propagation direction z and transversal dimension x . (c) Intensity oscillation owing to the Talbot effect at $x=0$ and $x=d/2$. (d) Numeric (solid curve) and analytic (dashed curve) calculations of the uniform field amplitude versus propagation direction. The oscillations result from nonlinear energy flow between the uniform and sinusoidal fields.

that the intensity modulation [Fig. 1(c)] is significant while the change in the amplitude of the uniform component [Fig. 1(d)], which is due to the energy exchange between the components, is much smaller.

We are now in a position to search for Talbot solitons. Since the energy flow between the components is small and its periodicity is much shorter than the diffraction and focusing length (~ 1 in normalized NLSE), we neglect the right-hand-side terms in Eqs. (3a) and (3b) and obtain

$$\frac{\partial \phi_1}{\partial y^2} + \left[\phi_1^2 + \frac{\phi_2^2}{2} \right] \phi_1 = \alpha_1 \phi_1, \quad (5a)$$

$$\frac{\partial \phi_2}{\partial y^2} + \left[\phi_2^2 + \frac{3\phi_1^2}{4} - k^2 \right] \phi_2 = \alpha_2 \phi_2. \quad (5b)$$

We solve Eqs. (5a) and (5b) by the self-consistent method [13]. An example of such a solution with $\phi_2(y=0) = 1$ and $\phi_1(y=0) = 0.2$ is shown in Fig. 2(a). Figure 2(b) shows the width of the two fields as a function of $\phi_1(y=0)$. We verified the stability of these solitons by simulating their propagation [using Eq. (1)] with 5% initial noise in amplitude and phase. An example of such a simulation with $\phi_2(y=0) = 1$, $\phi_1(y=0) = 0.2$, and $d = 0.5$ is shown in Fig. 3. The trapping of the soliton is displayed in Figs. 3(a)–3(d). Figure 3(e) shows the significant intensity modulation owing to the Talbot effect. Figure 3(f) shows the modulation of the amplitude of the uniform component. As shown, Eq. (4) correctly predicts the periodicity. However, it overestimates the amplitude of the oscillations because it does not take into account the reduced intensities at planes $y \neq 0$.

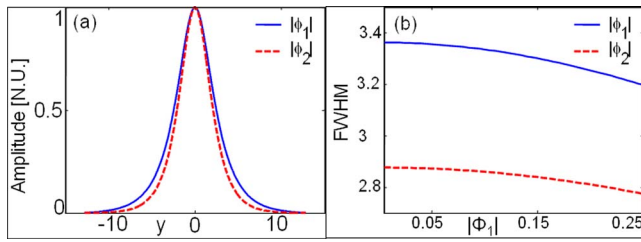


Fig. 2. (Color online) Talbot solitons wave functions. (a) Amplitude profiles of the uniform (solid curve) and sinusoidal (dashed curve) components of Talbot solitons with $\phi_2(0)=1$ and $\phi_1(0)=0.2$. (b) Amplitude FWHM of the uniform (solid curve) and sinusoidal (dashed curve) components as a function of the uniform component peak amplitude. The peak amplitude of the sinusoidal component is fixed to 1.

An exciting feature of Talbot solitons is that they can induce a 1D waveguide and a 2D photonic lattice within the waveguide. A possible application is utilizing Talbot solitons for enhancing the harmonic generation processes. Previous work employed solitons for enhancing second-harmonic generation by induc-

ing a waveguide for the driving and second-harmonic beams [14]. Talbot solitons open the possibility to induce both the waveguide and the index grating structure that can be used for grating-assisted quasi-phase matching of harmonic generation [15,16]. Another direction is using Talbot solitons for a narrow bandwidth optical filter, which can be tuned in real time by varying the soliton parameters. Soliton-induced waveguide filters are tunable in real time and robust against fabrication errors, index inhomogeneities, etc. Finally, it might be possible to wrap the Talbot strip soliton around itself [4] and the obtained ring Talbot soliton that induces a 2D photonic lattice in a 2D ring waveguide.

In conclusion, we propose a new type of optical solitons, Talbot solitons, which consists of sinusoidal and uniform components that are mutually coherent and jointly trapped in one direction. Talbot solitons induce a 1D waveguide and a 2D photonic lattice within the waveguide that may be used for quasi-phase matching of frequency conversion and for real-time tunable waveguide filters.

References

1. V. E. Zakharov and A. M. Rubenchik, *Sov. Phys. JETP* **38**, 494 (1974).
2. A. Barthelemy, S. Maneuf, and C. Froehly, *Opt. Commun.* **55**, 201 (1985).
3. C. Anastassiou, M. Soljacic, M. Segev, D. Kip, E. Eugenieva, D. N. Christodoulides, Z. H. Musslimani, and J. P. Torres, *Phys. Rev. Lett.* **85**, 4888 (2000).
4. M. Soljacic, S. Sears, and M. Segev, *Phys. Rev. Lett.* **81**, 4851 (1998).
5. O. Cohen, T. Carmon, M. Segev, and S. Odoulov, *Opt. Lett.* **27**, 2031 (2002).
6. J. R. Salgueiro, A. A. Sukhorukov, and Yu. S. Kivshar, *Opt. Lett.* **28**, 1457 (2003).
7. O. Cohen, M. M. Murnane, H. C. Kapteyn, and M. Segev, *Opt. Lett.* **31**, 954 (2006).
8. M. Haelterman, A. P. Sheppard, and A. W. Snyder, *Opt. Commun.* **103**, 145 (1993).
9. O. Cohen, R. Uzdin, T. Carmon, J. W. Fleischer, M. Segev, and S. Odoulov, *Phys. Rev. Lett.* **89**, 133901 (2002).
10. O. Cohen, S. Lan, T. Carmon, J. A. Giordmaine, and M. Segev, *Opt. Lett.* **27**, 2013 (2002).
11. M. Belic, Ph. Jander, A. Strinic, A. Desyatnikov, and C. Denz, *Phys. Rev. E* **68**, 025601 (2003).
12. C. Rotschild, O. Cohen, O. Manela, T. Carmon, and M. Segev, *J. Opt. Soc. Am. B* **21**, 1354 (2004).
13. M. Mitchell, M. Segev, T. Coskun, and D. N. Christodoulides, *Phys. Rev. Lett.* **79**, 4990 (1997).
14. S. Lan, M. Shih, G. Mizell, J. A. Giordmaine, Z. Chen, C. Anastassiou, J. Martin, and M. Segev, *Opt. Lett.* **24**, 1145 (1999).
15. M. M. Fejer, G. A. Magel, D. H. Jundt, and R. L. Byer, *IEEE J. Quantum Electron.* **28**, 2631 (1992).
16. S. Somekh and A. Yariv, *Appl. Phys. Lett.* **21**, 140 (1972).

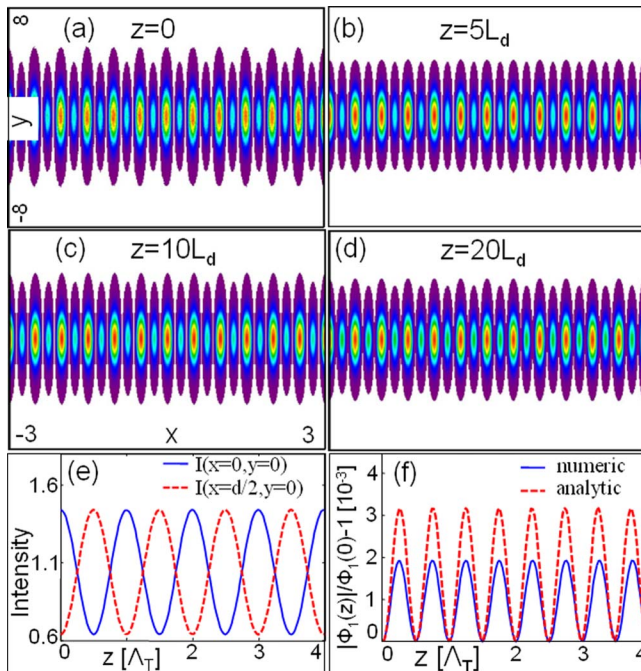


Fig. 3. (Color online) Talbot soliton. (a) Intensity of the beam launched into the medium in the presence of 5% noise; intensity of the beam after propagation of (b) 5, (c) 10, and (d) 20 diffraction lengths, showing that the beam is trapped in the y direction. (e) Intensity oscillation due to the Talbot effect at $(x=0, y=0)$ and $(x=d/2, y=0)$. (f) Numeric (solid curve) and analytic 1D model (dashed curve) calculation [Eq. (4)] of the uniform field amplitude versus propagation direction. The oscillations result from nonlinear energy flow between the uniform and sinusoidal fields.